Influence of NiO anode buffer layer prepared by solution on performance of bulk-heterojunction solar cells

Kyung Ho Kim[a,*], Chiaki Takahashi[a], Takashi Okubo[b], Yoshio Abe[a], Midori Kawamura[a]

[a] Department of Materials Science and Engineering, Kitami Institute of Technology, 165 Koen-cho, Kitami, Hokkaido 090-8507, Japan

[b] School of Science and Engineering, Kinki University, 3-4-1 Kowakae, Higashi-Osaka-shi, Osaka 577-8502, Japan

Abstract

We investigate the properties of NiO thin films prepared by sol-gel solution and the photovoltaic performance of bulk-heterojunction (BHJ) solar cells based on NiO thin films as anode buffer layers with various film thickness and amorphous-crystalline phase. Optoelectronic properties and surface morphology of NiO films strongly depend on the thickness and phase of the NiO. The performance of solar cells based on nanocrystaline (nc-) NiO exhibits better photovoltaic characteristics in comparison to those employing an amorphous (a-) NiO. The obtained power conversion efficiency (PCE, η) of a solar cell with a 20-nm-thick nc-NiO is 2.24%, with a short-circuit density

(J_{SC}) of 7.77 mA/cm^2, open-circuit voltage (V_{OC}) of 0.57 V, and fill factor (*FF*) of 0.50.

Keywords: Bulk-heterojunction solar cells, NiO, Anode buffer layer, Solution, Amorphous, Nanocrystalline

Corresponding author: Kyung Ho Kim, Tel: 81-157-26-9431, Fax: 81-157-26-4973,

E-mail address: khkim@mail.kitami-it.ac.jp

1. Introduction

Bulk-heterojunction (BHJ) solar cells have attracted attention due to their low weight, easy processing, cost-effectiveness, and flexibility as an alternative to conventional silicon-based solar cells [1-3]. The performance of BHJ solar cells is strongly related to an interfacial buffer layer between the active layer and the anode electrode [2,3]. Using poly(3,4-ethylenedioxythiophene) (PEDOT) doped with poly(styrene-sulfonate) (PSS), i.e., PEDOT-PSS, as an anode buffer layer has been investigated to further improve the cell performance [1,3,4]. Despite many positive effects, rapid degradation of the device performance occurred due to water absorption by the PEDOT:PSS layer and corrosion of the indium tin oxide (ITO) anode electrode in the device [5,6]. To overcome those issues, many effective approaches have been carried out through the wide bandgap oxide as an alternative anode buffer layer [5,7,8]. NiO is well known *p*-type transition metal oxide with low material cost, excellent durability, and electrochemical stability [9]. It was reported that NiO deposited by magnetron sputter or pulse layer deposition (PLD) could be used effectively to replace the PEDOT:PSS layer [6]. However, the defects caused by ion bombardment could degrade electrical performance and disrupt the surface structure during the sputtering process. Also, PLD is potentially applicable in large areas but could be plagued by

uneven coverage and high defect rates [10,11].

In this study, we investigated the fabrication and performance of NiO thin films prepared by sol-gel and the photovoltaic properties of BHJ solar cells based on NiO as anode buffer layers. NiO film thickness and crystalline phase play an important role in device performance. The sol-gel solution process provides the possibility of significant cost reduction via mass-manufacturing roll-to-roll processes using a combination of conventional coating and printing techniques [12,13].

2. Experimental

NiO thin films were prepared by the sol-gel method. Nickel acetate tetrahydrate $Ni(Ac)_2 \cdot H_2O$ as a precursor was dissolved in 2-methoxyethanol and hydrochloric acid (HCl) was added as catalyst [14]. The solution was stirred at 60 ^{o}C for 1 h, and then aged for 24 h at room temperature [14]. Glass and ITO (10 Ω/sq.) coated glass (Geomatec Co., Ltd.) substrates were used. They were subjected to a standard cleaning process with acetone, isopropyl alcohol and deionized water for 10 min each, in an ultrasonic bath.

NiO thin films with different thickness were prepared by a spin-coating technique with various spin-speeds and times. After spin-coating, the films were oxidized at 350

^{o}C for 5 min in air [14]. Then, one was annealed at 450 ^{o}C for 1 h using a hot plate, and the other was annealed in a furnace at 450 ^{o}C for 1 h with a heating rate of 5 ^{o}C/min in ambient air, respectively.

The BHJ solar cells were fabricated using conventional processes as shown in Fig. S1. An active layer of poly-(3-hexylthiophene) (P3HT):[6,6]-phenyl C_{61} butyric acid methyl ester (PCBM) (chlorobenzene solution of 1:0.75 wt.%) was cast to be 110 nm on top of the NiO film and annealed at 150 ^{o}C for 0.5 h in a nitrogen glovebox. Then, an LiF hole blocking layer and Al cathode electrode were evaporated with about 0.7 nm and 70 nm thickness, sequentially.

Films thickness was measured by variable-angle ellipsometry (MIZOJIRI, DVA-FL). Resistivity and ultraviolet-visible (UV-Vis) spectroscopy (HITACHI, U-2910) were carried out. The structure of the NiO films was examined through X-ray diffraction (XRD, Bruker, D8ADVANCE) using a 2θ scan. The surface morphologies were investigated by atomic force microscopy (AFM, SHIMADZU, SPM-9500J3) and scanning electron microscopy (SEM, JSM-6701F).

The photovoltaic properties of solar cells were measured at room temperature under AM 1.5G (100 mW/cm^2) provided by a solar simulator (OTENTOSUN-3RK). The cell area was 6 mm^2.

3. Results and Discussion

3.1. Film properties of NiO

Figure 1 shows the resistivity and transmittance with various NiO films on glass substrates annealed using a hot plate. The resistivity of 5-nm-thick NiO film is too high to measure, and it decreases with increase in film thickness as seen in Fig. 1. Compared with the NiO prepared by reactive sputtering [5], the resistivity of NiO prepared by solution is relatively high.

The transmittance of 5-nm-thick NiO is above 90%, indicating that it is highly transparent near the P3HT:PCBM active layer main absorption peak of 520 nm, and it decreases with increasing NiO thickness. As NiO thickness increases up to 40 nm, the absorbance of NiO film in the visible range cannot be ignored as seen in Fig. S2 (a) of the supporting information. As the anode buffer layer in BHJ solar cells, it usually requires high transparency and low resistivity.

The XRD patterns with various NiO films are shown in Fig. 2. NiO films are regarded as amorphous (a-) phase because no significant crystalline peaks are observed. The effects of NiO phase on photovoltaic characteristics of BHJ solar cells were not clearly observed.

Figure 3 shows the root mean square (rms) roughness of a-NiO films. The rms

roughness is about 6.1 nm for 5-nm-thick a-NiO, which is similar in value compared to that of the bare ITO/glass substrate without annealing. However, it is smoother in comparison to the rms value (8.3 nm) of ITO annealed at 450 ^{o}C using a hot plate (see Fig. S5). With increasing a-NiO thickness, the rms roughness reduces down to 2.1 nm, becoming smoother. It is well known that surface roughness plays an important role in the interface properties of devices [3]. It may be also related to the decrease in optical bandgap (E_g) of a-NiO with increase in thickness as shown in Fig. S2 (a). The obtained value of E_g matches well with the value reported by others [15, 16]. It was also reported that the E_g of NiO thin films prepared by the spray pyrolysis technique slightly decreases with increasing film thickness [9].

3.2. Photovoltaic characteristics of BHJ solar cells with a-NiO buffer layers

Figure 4 shows the photocurrent density–voltage (J–V) curves of solar cells based on various a-NiO films. It is clearly shown that the short-circuit current density (J_{SC}) and open-circuit voltage (V_{OC}) of solar cells change with increase in the NiO thickness. The details of parameters, J_{SC}, V_{OC}, fill factor (FF), power conversion efficiency (PCE, η), and series resistance (R_S) of the cells are summarized in Table 1. J_{SC} increases up to 7.23 mA/cm^2, for solar cells based on a 20-nm-thick a-NiO film, and declines with

further increase in thickness of the NiO films. This is because the light absorption in 40-nm-thick NiO increases (see Fig. S2), which leads to a decrease in the number of excitons generated in the active layer. However, 5 nm and 10 nm a-NiO films show too high a resistivity. Therefore, combined effects of the absorption and resistivity of the a-NiO films induce the J_{SC} variation of BHJ solar cells.

It is observed that V_{OC} increases from 0.39 V to 0.55 V when NiO thickness changes from 5 nm to 20 nm, and saturates for thicker NiO films. It is well known that V_{OC} of BHJ solar cells depends on 1) the difference between the highest occupied molecular orbital (HOMO) level of donor and the lowest unoccupied molecular orbital (LUMO) level of acceptor, and 2) the work function difference between anode and cathode metal [17]. It was also reported that V_{OC} slightly changed with the electrical properties of the PEDOT:PSS anode buffer layer [3]. It could be assumed that V_{OC} could be further improved by optimizing the condition of the anode buffer layer.

The variations of the *FF* of the solar cells with a-NiO films are similar to those of J_{SC}. The lowest R_S, calculated from the inverse slope at V_{OC} [1], is obtained from BHJ solar cells based on the 20-nm-thick a-NiO compared with that of solar cells employing the films of other thicknesses. As a result, the overall conversion efficiency of BHJ solar cells with 20 nm a-NiO film is enhanced due to the improved photocurrent density,

V_{OC}, and *FF* with relatively low R_S.

3.3. Influence of nanocrystalline (nc-) NiO

Figure 5 shows the XRD of 20-nm-thickness NiO films annealed by furnace. It is clearly observed that crystalline peaks occur at 37.25° for (111) and 43.28° for (200) corresponding to NiO (JCPDS no. 01-1239). The average nanocrystalline size is ~ 20 nm as seen in Fig. S7. Control of the heating rate is an effective way to modify the crystallinity of films [18]. However, using sol-gel method, it is needed still high processing temperature compared that of conventional PEDOT-PSS. It could be decreased using such as a solvent with relatively low boiling temperature, adding additional catalyst, and so on.

Carrier transfer from the active layer to the anode electrode correlates with the mobility of the anode buffer layer, and this could be expected to improve the cell performance. It has been reported that the hole mobility of NiO prepared by sputtering increased with heat treatment [16].

Figure 6 shows *J-V* curves of solar cells based on nc-NiO as anode buffer layers. J_{SC} is 7.77 mA/cm^2, which is a 7.4% increase compared to that of a solar cell with 20 nm a-NiO film. It could be related to the slightly better transmittance of nc-NiO film

compared with that of a-NiO (see Fig. S3). It was reported that the nc-oxide semiconductor, compared with a-oxide semiconductor, exhibited better optical properties in the visible range [19]. The V_{OC} of the cells with nc-NiO film is slightly enhanced (to 0.57 V) with respect to that of a-NiO based solar cells of comparable film thickness. The R_S of a solar cell with nc-NiO film is 16.10 Ω·cm^2, leading to a 16.2% increase in the *FF* (to 0.51). It reflects well that the relatively low resistivity (~ 35 Ωcm) and smooth surface roughness are comparable to that of a-NiO (see Fig. S6). The obtained efficiency (2.24%) of BHJ solar cells based on the nc-NiO is improved mainly due to an increase in photocurrent and fill factor.

4. Conclusions

The properties of NiO films prepared by solution are strongly dependent on thickness and heating methods. Using nc-NiO as an anode buffer layer of BHJ solar cells, the cells exhibits high efficiency with relatively high photocurrent density and a *FF* with low series resistance in comparison with solar cells based on a-NiO. It could be expected that optimizing conditions will lead to further improvement in the photovoltaic performance of nc-NiO-based BHJ solar cells.

References

[1] M. Ichikawa, E. Suto, H-G. Jeon, Y. Taniguchi, Sensitization of organic photovoltaic cells based on interlayer excitation energy transfer, Org. Electron. 11 (2010) 700-704.

[2] T-S. Huang, C-Y. Huang, Y-K. Su, J-S. Fang, M. V. M. Rao, T-F. Guo, T-C. Wen, High-efficiency polymer photovoltaic devices with glycerol-modified buffer layer, IEEE Photon. Technol. Lett. 20 (2008) 1935-1937.

[3] S.H. Eom, S. Senthilarasu, P. Uthirakumar, S.C. Yoon, J. Lim, C. Lee, H.S. Lim, J. Lee, S-H Lee, Polymer solar cells based on inkjet-printed PEDOT:PSS layer, Org. Electron. 10 (2009) 536-542.

[4] J. Li, S. Kim, S. Edington, J. Nedy, S. Cho, K. Lee, A. J. Heeger, M. C. Gupta, J. T. Yates Jr, A study of stability of P3HT/PCBM organic solar cells by photochemical active TiO_x layer, Sol. Energy Mater. Sol. Cells 95 (2011) 1123-1130.

[5] R. Betancur, M. Maymo, X. Elias, L.T. Vuong, J. Martorell, Sputtered NiO as electron blocking layer in P3HT:PCBM solar cells fabricated in ambient air, Sol. Energy Mater. Sol. Cells 95 (2011) 735-739.

[6] M.D. Irwin, D.B. Buchholz, A.W. Hains, R.P.H. Chang, T.J. Marks, p-Type semiconducting nickel oxide as an efficiency-enhancing anode interfacial layer in

polymer bulk-heterojunction solar cells, Proc. Natl. Acad, Sci. 105 (2008) 2783-2787.

[7] V. Shrotriya, G. Li, Y. Yao, C-W. Chu, Y. Yang, Transition metal oxides as the buffer layer for polymer photovoltaic cells, Appl. Phys. Lett. 88 (2006) 073508-1-3.

[8] S. Han, W.S. Shin, M. Seo, D. Gupta, S-J. Moon, S. Yoo, Improving performance of organic solar cells using amorphous tungsten oxides as an interfacial buffer layer on transparent anodes, Org. Electron. 10 (2009) 791-797.

[9] P.S. Patil, L.D. Kadam, Preparation and characterization of spray pyrolyzed nickel oxide (NiO) thin films, Appl. Surf. Sci. 199 (2002) 211-221.

[10] H. Yabuta, M. Sano, K. Abe, T. Aiba, T. Den, H. Kumomi, K. Nomura, T. Kamiya, and H. Hosono, High-mobility thin-film transistor with amorphous $InGaZnO_4$ channel fabricated by room temperature rf-magnetron sputtering, Appl. Phys. Lett. 89 (2006) 112123-1-3.

[11] R.C. Ross and R. Messier, Microstructure and properties of rf-sputtered amorphous hydrogenated silicon films, J. Appl. Phys. 52 (1981) 5329-5339.

[12] T. Shimoda, Y. Matsuki, M. Furusawa, T. Aoki, I. Yudasaka, H. Tanaka, H. Iwasawa, D. Wang, M. Miyasaka, and Y. Takeuchi, Solution-processed silicon films

and transistors, Nature 440 (2006) 783-786.

[13] B.S. Ong, C. Li, Y. Li, Y. Wu, and R. Loutfy, Stability, solution-processed, high-mobility ZnO thin-film transistors, J. Am. Chem. Soc. 129 (2007) 2750-2751.

[14] Z. He, Z. Ji, S. Zhao, C. Wang, K. Liu, Z. Ye, Characterization and electrochromic properties of $Cu_xNi_{1-x}O$ films prepared by sol-gel dip-coating, Sol. Energy 80 (2006) 226-230.

[15] A.S. Nandy, B. Saha, M.K. Mitra, and K.K. Chattopadhyay, Effect of oxygen partial pressure on the electrical and optical properties of highly (200) oriented p-type $Ni_{1-x}O$ films by DC sputtering, J. Mater. Sci. 42 (2007) 5766-5772.

[16] M. Guziewicz, J. Grochowski, M. Borysiewicz, E. Kaminska, J.Z. Domagala, W. Rzodkiewics, B.J. Witkowski, K. Golaszewska, R. Kruszka, M. Ekielski, A. Piotrowska, Electrical and optical properties of NiO films deposited by magnetron sputtering, Optica Applicata, XLI (2011) 431-440.

[17] A. Moliton, J-M. Nunzi, How to model the behavior of organic photovoltaic cells, Polym Int. 55 (2006) 583-600.

[18] J. Zhang, Y. Yang, B. Xu, F. Jiang, J. Li, Shape-controlled synthesis of ZnO nano- and micro-structures, J. Cryst. Grwoth 280 (2005) 509-515.

[19] K.H. Kim, G.H. Kim, H.J. Kim, Fabrication of transparent nanocrystalline $InGaO_3(ZnO)_2$ thin films using a solution process, Phys. Status Solidi A 207 (2010) 1660-1663.

Table 1. Photovoltaic properties of BHJ solar cells as a function of NiO thickness under AM 1.5 illumination condition.

Thickness (nm)	J_{SC} (mA/cm^2)	V_{OC} (V)	FF -	η (%)	R_S (Ω·cm^2)
5	1.61	0.39	0.38	0.25	94.20
10	4.90	0.45	0.40	0.89	49.90
20	7.23	0.55	0.43	1.70	27.30
40	6.30	0.55	0.39	1.35	38.40
*20	7.74	0.57	0.51	2.24	16.10

* DSSCs with 20-nm-thick nc-NiO

Figure Captions

Fig. 1. Resistivity (solid squares) and transmission (empty squares) at a wavelength of 520 nm as a function of NiO thickness.

Fig. 2. XRD patterns with various NiO films on glass substrates annealed using hot plate.

Fig. 3. Root mean square (rms) roughness of different a-NiO films on ITO/glass substrates annealed using hot plate.

Fig. 4. Photocurrent density–voltage (*J*-*V*) curves of BHJ solar cells based on various a-NiO films.

Fig. 5. XRD pattern of 20-nm-thick NiO film on glass annealed at 450 ^{o}C using furnace with heating rate of 5 ^{o}C/min.

Fig. 6. J-V curve of BHJ solar cell employing the nc-NiO film.

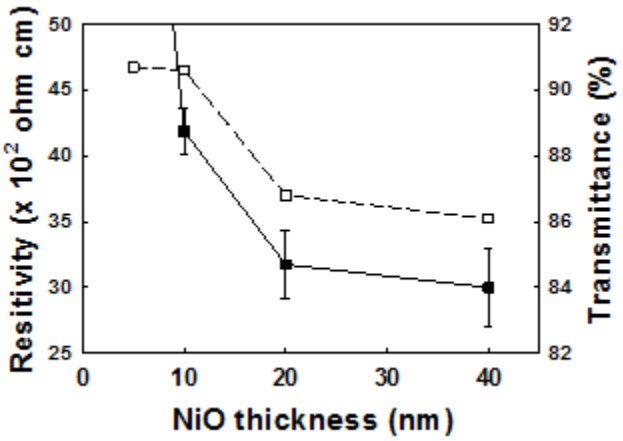
Resitivity (x 10^2 ohm cm)
Transmittance (%)
NiO thickness (nm)
50
45
40
35
30
25
92
90
88
86
84
82
0
10
20
30
40

Fig. 1.

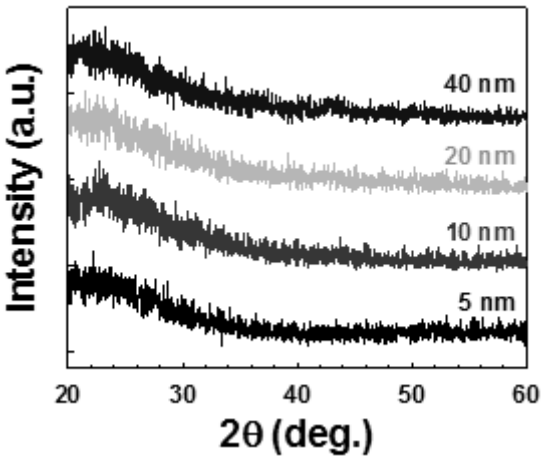

Fig. 2.

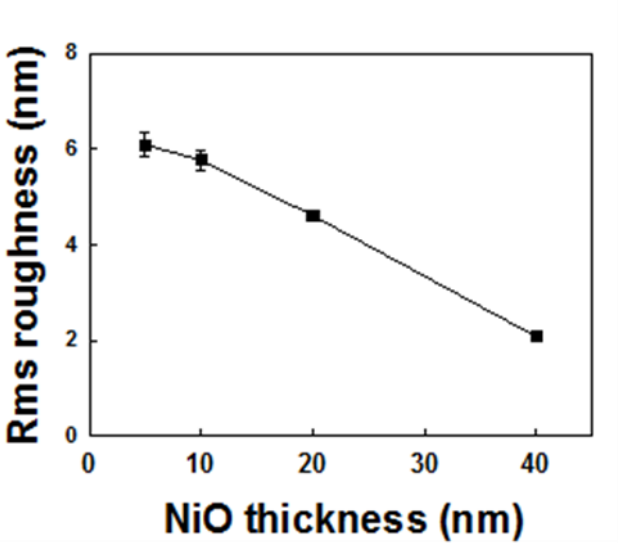

Fig. 3.

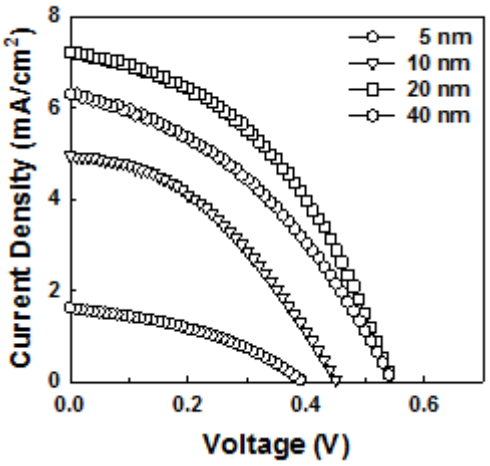
Current Density (mA/cm^2)
Voltage (V)
5 nm
10 nm
20 nm
40 nm
0
2
4
6
8
0.0
0.2
0.4
0.6

Fig. 4.

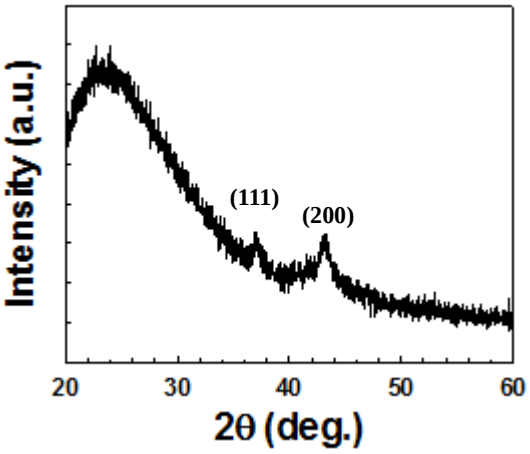

Fig. 5.

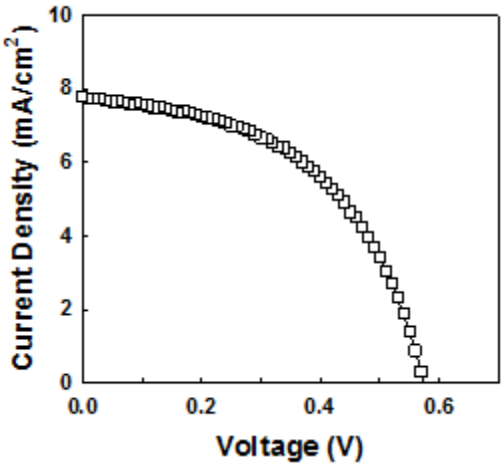

Fig. 6.